IEEE Access
Multidisciplinary | Rapid Review | Open Access Journal

SPECIAL SECTION ON IEEE ENGINEERING IN MEDICINE AND BIOLOGY SOCIETY SECTION

Received 17 April 2023, accepted 6 May 2023, date of publication 10 May 2023, date of current version 18 May 2023.

Digital Object Identifier 10.1109/ACCESS.2023.3275015

RESEARCH ARTICLE

Intelligent Stethoscope System and Diagnosis Platform With Synchronized Heart Sound and Electrocardiogram Signals

SHUENN-YUH LEE[1], (Senior Member, IEEE), PO-HAN SU[1], (Student Member, IEEE), YI-TING HSIEH[1], (Graduate Student Member, IEEE), SHENG-HSIN HUANG[1], I-PEI LEE[2], AND JU-YI CHEN[3]

[1]Department of Electrical Engineering, National Cheng Kung University, Tainan City 70101, Taiwan
[2]National Cheng Kung University Hospital, National Cheng Kung University, Tainan City 70101, Taiwan
[3]Department of Internal Medicine, National Cheng Kung University Hospital, College of Medicine, National Cheng Kung University, Tainan City 70101, Taiwan

Corresponding authors: Shuenn-Yuh Lee (ieesyl@mail.ncku.edu.tw) and Ju-Yi Chen (juyi@mail.ncku.edu.tw)

This work was supported in part by the Taiwan Semiconductor Research Institute; in part by the Ministry of Science and Technology (MOST); and in part by the National Science and Technology Council (NSTC), Taiwan, under Grant MOST 111-2221-E-006-194, Grant NSTC 111-2634-F-006-012, and Grant NSTC 112-2622-8-006-009-TE1.

This work involved human subjects or animals in its research. Approval of all ethical and experimental procedures and protocols was granted by the Institutional Review Board of National Cheng Kung University Hospital under IRB No. B-BR-107-008, and performed in line with the Human Study Amendment Approval.

ABSTRACT This paper proposes an intelligent stethoscope system that synchronously displays the electrocardiogram (ECG) and heart sound. The instrument, which accelerates auscultation, can be used for the diagnosis of valvular heart disease (VHD) for clinical physicians. The whole system with ECG patch and stethoscope includes four parts, namely, an analog front-end circuit for bio-signal acquisition, a heart sound-classifying integrated circuit with convolution neural network (CNN), a user-friendly application that synchronously displays the heart sound and ECG signals, and a cloud server with heart murmur detection algorithm for human study. In this system, three algorithms are used in processing both ECG and heart sound signals. The first algorithm is a synchronized algorithm, which can align heart sound and ECG signals simultaneously. The second algorithm is a heart sound-classifying algorithm that can distinguish the first (S1) and the second (S2) heart sound in heart sound signals for identifying the systolic and diastolic phases. The accuracies of the algorithm applied to normal heart sound and heart murmur are 100% and 96.7%, respectively. The third algorithm is heart murmur identification, which can detect systolic murmur and has a macro f1 score of 92.5%. The three algorithms proposed are beneficial for physicians in the diagnosis of VHD. After the establishment of the whole system, a CNN-based classification algorithm is also implemented with a 0.18 μm standard CMOS process for the demonstration of the edge computing. The machine learning techniques are implemented on the chip to accelerate the classification process.

INDEX TERMS Bio-signal acquisition, cardiac auscultation, electrocardiogram, heart sound, machine learning, application software, edge computing, stethoscope, murmur identification.

I. INTRODUCTION

The official statistics of the World Health Organization show that cardiovascular diseases (CVD) are the primary causes of death in 2019 [1], and they can be attributed to unhealthy lifestyles. Approximately 15% of elders suffer from valvular heart disease (VHD) [2], and 10% of congenital heart disease cases are caused by congenital valvular defects [3]. Severe VHD is life-threatening and affects patients in their entire lifetimes. VHDs are commonly caused by

The associate editor coordinating the review of this manuscript and approving it for publication was Sung-Min Park.

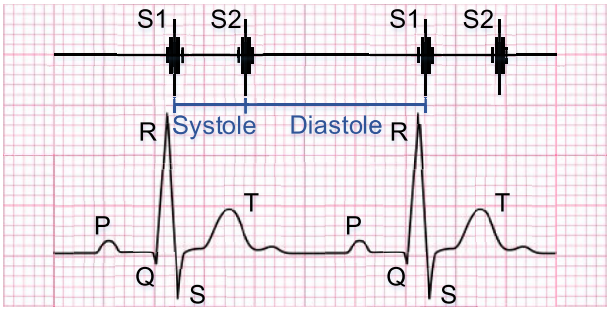

FIGURE 1. Association between the visualized heart sound and the ECG signal.

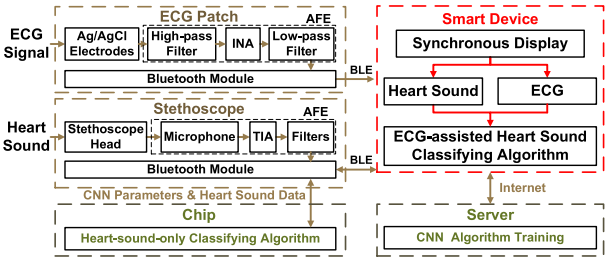

FIGURE 2. Structure of the proposed intelligent stethoscope system.

degeneration, rheumatic fever, congenital defect, and infection. These diseases are detected by collecting the bio-signal of a person for a long-time trace. Among all kinds of bio-signals, electrocardiography (ECG) is the most significant signal for monitoring cardiac electric activity. It is commonly used by doctors in CVD diagnosis. To preliminarily diagnose VHD, doctors generally perform auscultation.

Figure 1 shows the association between the visualized heart sound and the ECG signal. The first heart sound (S1), which appears near the R peak of the ECG signal, is produced when the atrioventricular valves close after the atriums eject blood into the ventricles. The second heart sound (S2), which appears at the end of the T wave, is generated by the closing of the aortic and pulmonary valves after the ventricles pump blood into the artery. The interval from S1 to S2 is the duration of ventricular contraction, called systole. The period from S2 to S1 is the time interval of ventricular relaxation, called diastole. The time interval of diastole is usually longer than that of systole because the blood needs more time to flow back to the heart.

Mitral regurgitation (MR) and aortic stenosis (AS) are the two common systolic heart murmurs. MR is produced by the abnormal closing of the mitral valves. Blood refluxes from the left ventricle to the left atrium during ventricular contraction, and the best auscultation area for MR is the mitral area. AS originates from the abnormal opening of aortic valve. AS indicates that blood is forced to eject through a tiny path. The intensity of AS is different from that of MR. Its intensity initially increases, and then decreases during systole. The best auscultation area for AS is the aortic area.

Since the valve condition is closely related to heart sounds, doctors can preliminarily diagnose VHD with a stethoscope. The stethoscope can collect heart, lung, and vascular flow sounds from the four areas for auscultation, namely the aortic, pulmonic, tricuspid, and mitral areas [4]. Although auscultation can be used for the diagnosis of VHD, doctors must have outstanding listening ability, rich clinical experience, the ability to distinguish the locations of S1 and S2 rapidly and accurately, and capability of identifying systole and diastole murmurs during a cardiac cycle. These issues are crucial to auscultation, but junior physicians who are not well-trained cardiologists may have difficulties in learning the skill of auscultation. Moreover, the diagnosis of heart sound is subjective. Even for the considerable experience of cardiologists, they are prone to express their views on heart sound through subjective words. Therefore, modern electronic stethoscopes [4] have become powerful tools for auscultation. Electronic stethoscopes can convert the analog signals of acoustic sounds into digital data for computer processing. Through years of hard work on heart sound signal processing [5], [6], [7], [8], [9], auscultation with computer-aided engineering has attracted research interest. However, the methods for real-time signal processing are complex, and signal quality is prone to be affected by environmental noise. Other causes, such as distinct sound level, age, and body type, influence the accuracy of auscultation. Therefore, valid identification through a heart-sound-only algorithm is hard to achieve.

In this work, the proposed system can visualize the heart sound signal and synchronize it with the ECG signal, thus facilitating diagnosis through auscultation. Considering that the relationship between heart sound and ECG signals can contribute to distinguish S1 and S2 in heart sound signals by the ECG-assisted heart sound classification algorithm, the proposed system can achieve the telemedicine of auscultation and be used for clinical diagnosis. The main contributions of this paper can be summarized as follows. The proposed system includes hardware and software. A digital filter is developed to simulate the effect of the tube of a traditional stethoscope, and thus the tube can be removed. A synchronization algorithm is designed to synchronize the ECG and heart sound signals. An ECG-assisted algorithm and a heart-sound-only algorithm are proposed to classify S1 and S2. A wavelet-based algorithm is designed to detect heart murmurs. Additionally, clinical trials and reviews are conducted to evaluate the proposed system.

The rest of this paper is organized as follows. Section II introduces the hardware implementation of the proposed intelligent stethoscope, including heart sound and ECG acquisition circuits. Section III discusses the detailed algorithms of bio-signal synchronization, heart sound classification, and heart murmur detection. The implementation and measurement results of the prototype are introduced in Section IV. Section V describes the chip design of heart sound classifying algorithm. The measurement results of the chip are illustrated in Section VI. The comparison with

TABLE 1. Main specifications of the prototypes.

	Stethoscope	ECG Patch
Power	3.7 V Li-Ion battery (CP1654 A3)	
Operating voltage	3.3 V	
MCU	Arm Cortex-M4 built in the nRF52840 module	
Sampling rate	2 kHz	500 Hz
Resolution	16 bits	12 bits
Gain	10 kV/I provided by the TIA	300 V/V provided by the INA
Frequency band	20–300 Hz	0.02–150 Hz

state-of-the-art works is provided in Section VII. Finally, the conclusion is presented in Section VIII.

II. HARDWARE IMPLEMENTATION

Unlike conventional electronic stethoscopes [10], [11], [12] or ECG monitoring devices [13], [14], [15], [16], the proposed system is equipped with both the ECG and heart sound sensors, as shown in Figure 2. The system contains five blocks, namely, an ECG monitoring device (ECG patch), a heart sound monitoring device (stethoscope), a smart device application (APP) with a graphical user interface (GUI), a server for training CNN algorithm, and a chip with a heart-sound-only classifying algorithm. The ECG patch and stethoscope, each has a Bluetooth low-energy (BLE) module, can collect ECG signals from the human chest and heart sound signals at the required auscultation locations, respectively. To perform ECG-assisted heart sound classification, the acquired ECG and heart sound data are transmitted to the smartphone for processing and display. In addition, a heart sound classifying chip is implemented for the scenario where the additional cost and setup process of the ECG patch are not desired by the users. Moreover, if the smartphone is connected to the internet, the CNN parameters for the classifying chip can be renewed according to the revised coefficients from a cloud server with training algorithm. In this section, the design issues of the stethoscope and ECG patch are introduced.

A. STETHOSCOPE

As shown in Figure 2, the stethoscope consists of a 3M^{TM} Littmann® Master Cardiology^{TM} stethoscope's head, an analog front-end (AFE) circuit, an nRF52840 Bluetooth module with a built-in microcontroller unit (MCU), and a self-designed firmware. The commercial stethoscope's head confirms the quality of heart sound input to the AFE. The AFE circuit, which contains a POM-2738L microphone, a trans-impedance amplifier (TIA), a high-pass filter, and a low-pass filter, is responsible for converting and processing the heart sound to a voltage signal. The output signal of the AFE is sampled by the analog-to-digital converter (ADC) embedded in the Bluetooth module with a frequency of 2 kHz and 16-bit resolution.

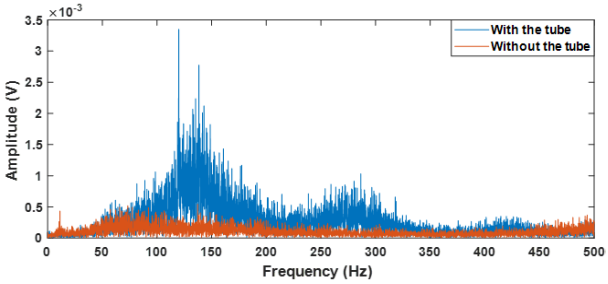

FIGURE 3. Frequency spectrum of the white noise sound measured with and without the tube.

The TIA in the AFE circuit is used to convert the current signal to voltage signal, because the output of the electret microphone is the current. The low-pass filter and high-pass filter are implemented with third-order Sallen-Key topology to remove out-of-band noise. The main specifications of the proposed stethoscope are summarized in Table 1. Considering that the latex tube used in a traditional stethoscope is no longer required for the proposed stethoscope, the frequency spectrum of the heart sound measured with the proposed stethoscope differs from that with the traditional stethoscope. Therefore, the frequency response model of the traditional stethoscope's tube is analyzed and implemented by a digital filter, called a tube filter, to process the heart sound signals and make the resulting signals fit in with the conventional characteristics of auscultation with stethoscope's tube for the convenient listening of cardiologist. To build the tube filter, a white noise sound is applied to the diaphragm, and the microphone of the proposed heart sound measuring circuit is placed at the earpieces or output terminal of stethoscope's head to measure the signals with or without the tube, respectively. By comparing the frequency spectrum of the signals, as shown in Figure 3, the tube is found to enhance the heart sound signal at the frequencies of approximately 140 Hz and 280 Hz in the desired frequency range of 20–300 Hz. Therefore, a 1000-tap finite impulse response filter is developed as the tube filter by Wiener-Hopf method to simulate the effect of the tube. The tube filter is implemented in the smart device and the cardiologists are not required to adapt their hearing between traditional and proposed stethoscopes on the diagnosis.

B. ECG PATCH

Figure 2 also shows the block diagram of the ECG patch, which consists of an AFE circuit, a Bluetooth module with MCU, and a self-designed firmware. Conventional Ag/AgCl electrodes are used to stick the ECG patch on the body and sense the ECG signal. The AFE circuit contains a high-pass filter, an instrumentation amplifier (INA), and a low-pass filter. Considering that ECG signals are measured with a two-electrode configuration, a simple passive high-pass filter

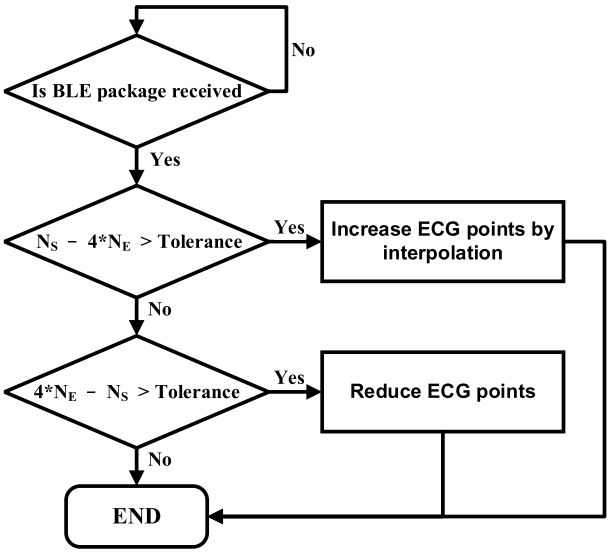

FIGURE 4. Flow chart of the synchronization algorithm for heart sound and ECG data.

is used to reduce the motional artifact. The INA is implemented to provide gain and convert the differential signal to a single-ended signal. The low-pass filter is implemented with second-order Sallen-Key topology to filter out undesirable high-frequency signals. After processing by the AFE, the ECG signal is sampled with a 500-Hz sampling rate and processed by the ADC with 12-bit resolution in the Bluetooth module. The main specifications of the proposed ECG patch are shown in Table 1.

III. SOFTWARE DESIGN

A. ALGORITHM FOR SYNCHRONIZING ECG AND HEART SOUND SIGNALS

S1 and S2 can be identified accurately, and systolic and diastolic heart murmurs can be distinguished by developing an algorithm with inputs of synchronous ECG and heart sound signals based on the relationship between PQRST waves and systole/diastole phases. However, considering that the devices used to measure ECG and heart sound signals are independent, the bio-signals are unsynchronous because of wireless transmission and BLE package loss. Accordingly, a synchronization algorithm should be designed. In the synchronization algorithm, the characteristic, in which the sampling rate of heart sound signal is four times larger than that of ECG signal, is used as the index to synchronize the ECG and heart sound signals. Whenever the software receives the data package with BLE, the algorithm checks the quantitative relationship between ECG and heart sound signals. For unsynchronized relationship, the heart sound data are regarded as golden data and compared with the ECG data. If the heart sound data are lost, extra ECG data are omitted. If ECG data are lost, the quantity of ECG data is increased with an interpolation method. Figure 4 shows the flow chart of the synchronization algorithm for heart sound and ECG data,

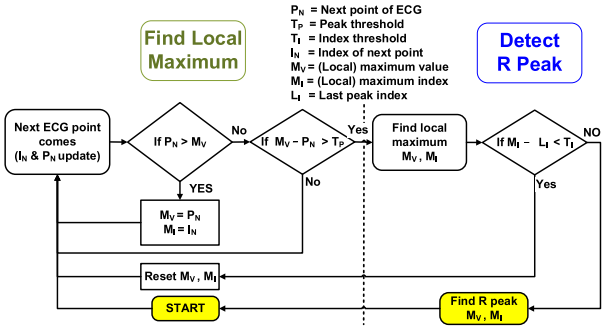

FIGURE 5. Flow chart of ECG R peak detection algorithm.

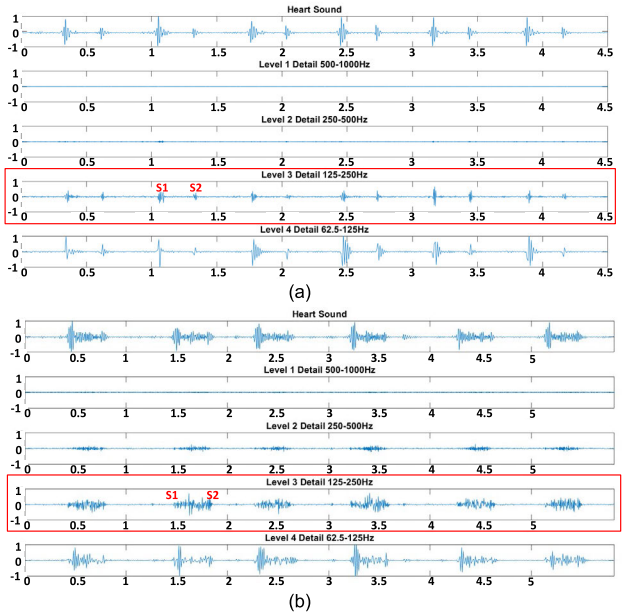

FIGURE 6. Heart sound with wavelet analysis: (a) Normal heart sound. (b) Systolic heart murmur, MR.

where N_E is the number of ECG data, and N_S represents the number of heart sound data. Considering that the sampling rate of a heart sound signal is designed to be four times larger than that of an ECG signal, four times the quantity of N_E should be equal to N_S for the alignment of both signals. Tolerance is associated with a delay of 0.1 s between ECG and heart sound signals and can be redefined in clinical trials.

B. S1 AND S2 ECG-ASSISTED HEART SOUNDS CLASSIFICATION

The classification algorithm is designed for distinguishing S1 and S2 in heart sound signals, and it consists of three steps. First, the R peaks of ECG signals are detected using the algorithm illustrated in Figure 5. Next, the heart sound peaks are recognized according to the energy of heart sound and the comparison with a defined energy threshold, which can be customized by a software. The energy of heart sound is calculated based on the formula of Shannon energy [17]

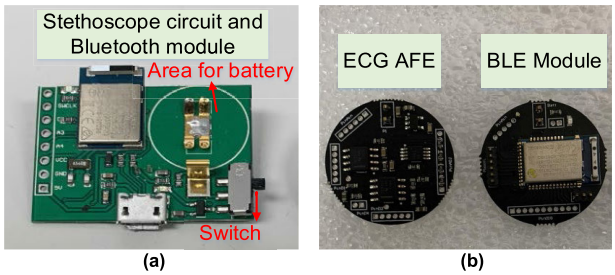

FIGURE 7. PCB of the AFE circuit and Bluetooth module. (a) The proposed stethoscope. (b) The proposed ECG patch.

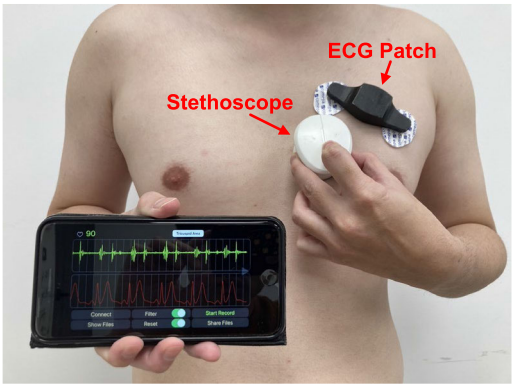

FIGURE 8. Measurement scenario of the proposed system.

shown in (1) and normalized to a range between 1 and −1.

$$\text{Shannon Energy} = -x^2 \times \log x^2 \tag{1}$$

Finally, the heart sound peaks are classified as S1 or S2 based on the occurrence timing of R peak in the synchronized ECG signal. Taking the occurrence timing of the ECG R peak as a reference, the valid timing ranges for classifying the heart sound peaks as S1 or S2 are shown in (2) and (3).

$$S1 : -40 - 120 \text{ ms} \tag{2}$$

$$S2 : 220 - 400 \text{ ms} \tag{3}$$

C. HEART MURMUR DETECTION

After S1 and S2 are detected, heart murmur should be further recognized for diagnosing the VHDs. The detection algorithm is designed to focus on recognizing the systolic murmur, because it commonly occurs on patients. The wavelet transform in [18] is used to analyze the characteristics of heart sounds. The result reveals that the frequency of murmur is higher than the frequencies of S1 and S2. Therefore, the murmur can be distinguished from normal heart sounds based on wavelet transform. Figure 6(a) shows that signals barely appear between S1 and S2 in the level 3 detail of normal heart sound. By contrast, in Figure 6(b), signals fill up the systolic phase of the heart sound because of the presence of MR murmur. In comparison with other levels of the wavelet transform, level 3 detail shows a clearer murmur than level 1 and 2 detail and a lower amplitude of S1 than level 4 detail.

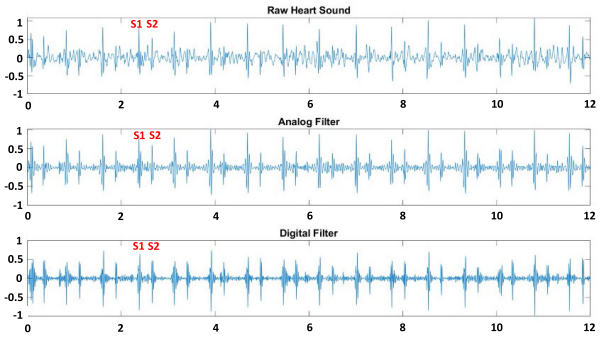

FIGURE 9. S1 and S2 identifications with proposed analog and digital filters.

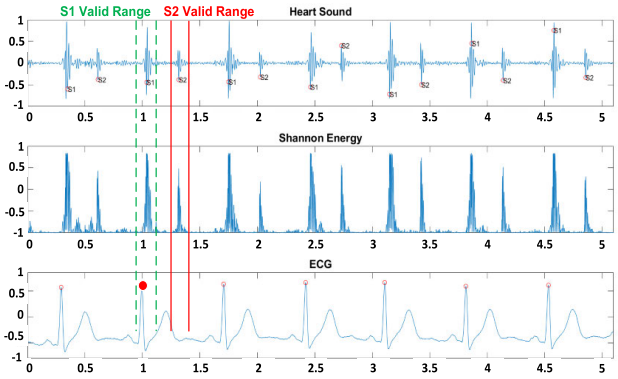

FIGURE 10. Result of heart sound classification algorithm and the example of indicated lines for S1, S2 classification.

Therefore, level 3 detail is chosen for identifying heart murmurs. After the S1 and S2 peaks are recognized, the timing range of murmur detection, which is the systolic phase, can be defined. The proposed algorithm combines the wavelet transform with the timing range of murmur detection to reach automatic murmur detection. The average energy of level 3 detail in the timing range of murmur detection is compared with an energy threshold to detect whether a heart murmur exists. If the average energy is greater than the threshold, a heart murmur is found. In contrast, the heart sound is normal if the average energy is lower than the threshold.

IV. IMPLEMENTATION AND MEASUREMENT RESULTS OF THE PROTOTYPES

A. STETHOSCOPE AND ECG PATCH

Figure 7(a) shows the printed circuit board (PCB) of the proposed stethoscope. The PCB contains an AFE circuit mentioned in Section II, a BLE module, an area for battery, a switch, and a charging circuit. The PCB, the battery, and the traditional stethoscope's head are integrated with a shell as a prototype, which is shown as the stethoscope in Figure 8. The diameter of the proposed stethoscope is less than 65 mm.

The AFE and the BLE module for the ECG patch are implemented on two PCBs, as shown in Fig. 9(b). The PCBs can be combined with a battery and packaged as the prototype

TABLE 2. Accuracy of heart sound classification algorithm applied to normal heart sound.

Item	True	False	Accuracy
S1	187	0	100%
S2	187	0	100%
Total	374	0	100%

TABLE 3. Accuracy of heart sound classification algorithm applied to heart murmurs.

Item	True	False	Accuracy
S1	459	6	98.7%
S2	440	25	95%
Total	899	31	96.7%

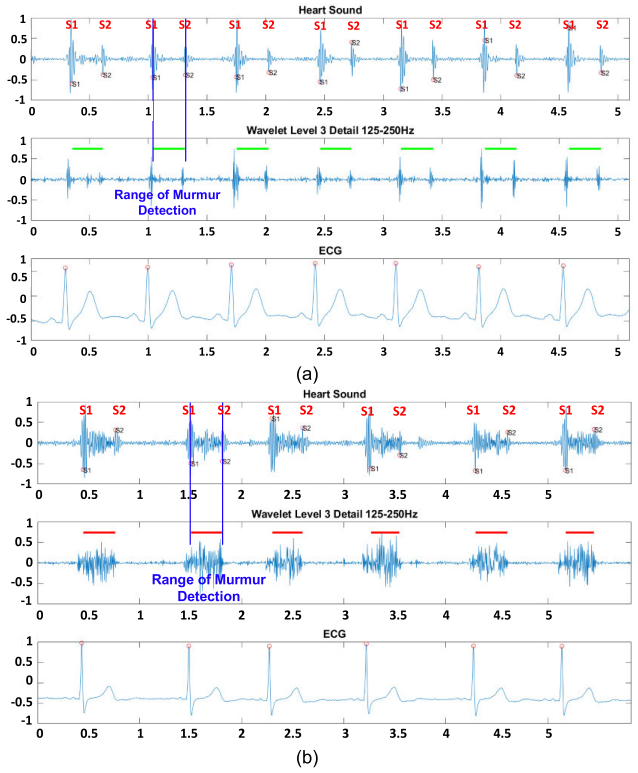

FIGURE 11. Heart murmur detection: (a) Normal heart sound. (b) Systolic heart murmur, MR.

ECG patch, which is shown as the ECG patch in Figure 8, for 24-hour ECG acquisition on the chest. The length of the ECG patch is 85 mm. Figure 8 shows the measurement scenario of the proposed system, which is similar to that of our previous work [19], but the wireless stethoscope and the ECG patch are independent.

As mentioned in Section II, the frequency response of latex tube is modeled with the digital filter in APP. Figure 9 shows the measurement results before and after filtering. The first row in Figure 9 shows that S1 and S2 are not clear in the raw heart sound signals, which is not filtered by the analog filters on the PCB. Especially, S2 mixes with low-frequency noise and becomes more difficult to be automatically distinguished

TABLE 4. Result of heart murmur detection.

Confusion Matrix		Actual		
		Murmur	Normal	Precision
Predicted	Murmur	420	8	98.1%
	Normal	33	179	84.4%
	Recall	92.7%	95.7%	

FIGURE 12. GUI of APP.

with the algorithm. The second row presents the clear S1 signal after analog filters with noise removal, but the signal is insufficiently sharp and cannot be used in distinguishing signals when murmur occurs. The third row shows the data processed by the digital filter, which are clear and suitable for heart disease identification because of the enhanced S1 and S2 signals.

B. S1 AND S2 HEART SOUND CLASSIFICATION AND HEART MURMUR DETECTION

Figure 10 shows the result of the application of heart sound classification on the clinical trial data. The segments between the dotted lines indicate valid ranges of S1, while solid lines indicate valid ranges of S2. These lines are determined based on the ECG R peak and the specifications in (2) and (3). Tables 2 and 3 list the detection accuracy of the proposed heart sound classification algorithm when applied to normal heart sound signals and heart murmurs, including AS and MR. The data are collected from the clinical trial of 18 patients without atrial fibrillation irregular beats in National Cheng Kung University Hospital (NCKUH). The NCKUH Institutional Review Board approved this research (IRB No. B-BR-107-008), and all the patients participating this clinical trial have provided their informed consents.

After locating S1 and S2, the algorithm further calculates level 3 detail data through wavelet analysis and checks whether murmur energy exceeds the defined threshold. Figure 11 shows the difference between the wavelet analysis results of normal heart sound and MR. The confusion matrix of heart murmur detection is provided in Table 4. The algorithm can achieve a precision of 98.1% and recall of 92.7% for heart murmur detection.

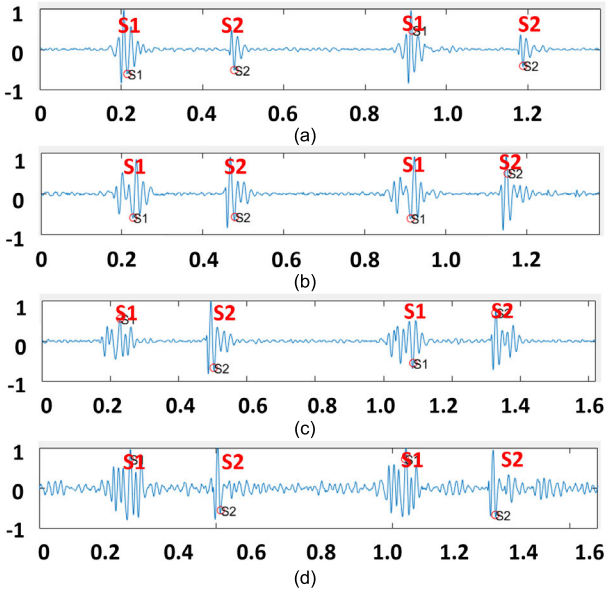

FIGURE 13. Normalized normal heart sound signals of a subject measured on different auscultation sites: (a) mitral area, (b) tricuspid area, (c) pulmonary area, and (d) aortic area.

C. GRAPHICAL USER INTERFACE (GUI)

The GUI is shown in Figure 12. The top channel presents the visualized heart sound waveform, and the bottom channel displays the ECG signal. The GUI makes the S1 and S2 of the top channel easily distinguished. Several function buttons are listed at the bottom for the control of reviewers. The top of the interface has a block, which can be controlled by the reviewers and shows the auscultation location for assisting the cardiologists in further off-line analysis.

D. HUMAN STUDY

In this work, the data are collected from 44 patients by using the proposed intelligent stethoscope system in NCKUH. The process of the clinical trial includes the following steps. First, the ECG patch and stethoscope are powered-up, and the ECG patch is attached to the patient with Ag/AgCl electrodes. Second, the self-designed APP is connected to the ECG patch and the stethoscope through Bluetooth. Then the received ECG and heart sound data are recorded and processed in APP. Finally, the physician places the stethoscope on the patient and diagnoses by observing the waveforms shown on the smart device and listening to the heart sound played with earphones. Data from 26 patients are used for testing the Bluetooth firmware and tube filter design. Data from the 18 remaining patients are used for the analysis of heart sound with the proposed algorithms. These 18 data can be separated into three groups. The first group contains five data with AS. The second group contains seven data with MR, and the third group contains six data with normal heart sound. Auscultation site influences human study intensively and should be accounted for. Figure 13 shows the heart sound signals collected using the proposed intelligent stethoscope system on four different sites. The result reveals that the heart sound

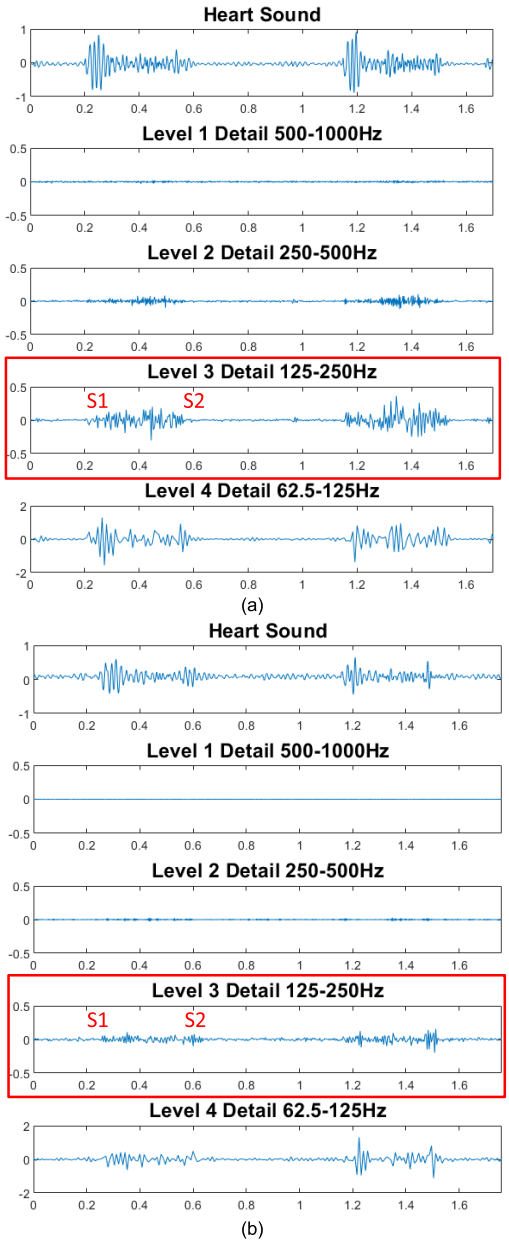

FIGURE 14. Wavelet analysis of MR on different auscultation site: (a) Mitral area (b) Tricuspid area.

signals measured on the mitral area has the largest amplitude ratio of S1 to S2, and the ratio gradually decreases according to the auscultation sites, as shown in Figures 13(a)–(c). Moreover, considering that the heart sound signals measured on the aortic area is generally small, the noise becomes obvious after normalization. In addition to S1 and S2, heart murmurs are also related to auscultation sites. According to the data of heart sound, the murmur of MR collected on the mitral area is louder than that collected on the tricuspid area, as shown in Figure 14. Moreover, the characteristic of MR, which is a holo-systolic murmur, can be found in the result of level 3 detail. This condition is beneficial for the identification of MR. Figure 15 shows that the loudest AS murmur occurred

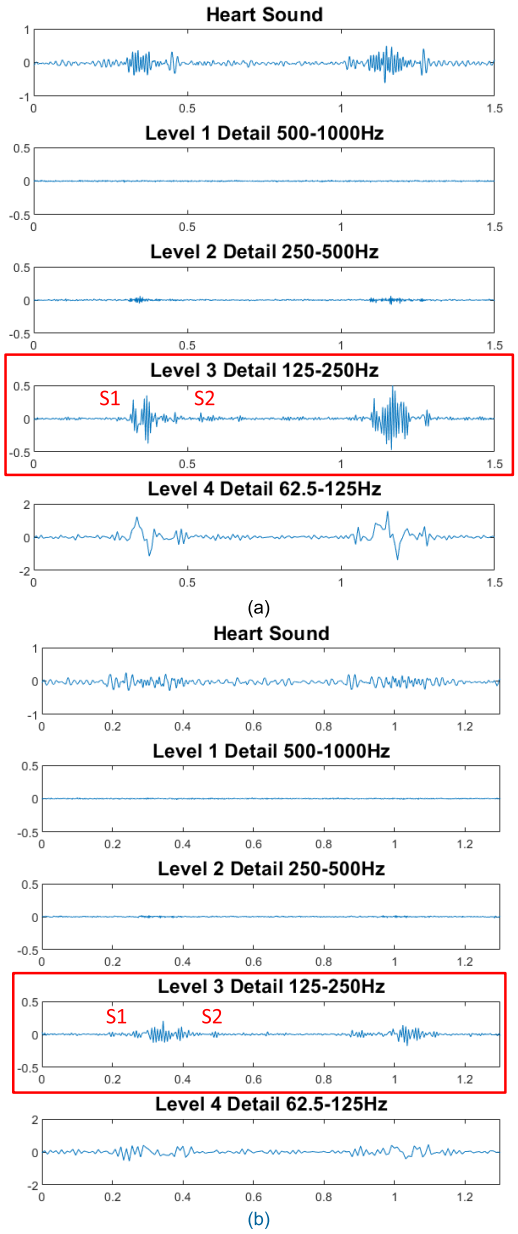

FIGURE 15. Wavelet analysis of AS on different auscultation site: (a) Aortic area (b) Mitral area.

in the aortic area, and the graph for the detected murmur has a diamond shape, as shown in Figure 15(a). These characteristics can be used in identifying the heart murmur of AS. As a result, the proposed intelligent stethoscope system preserves the characteristics of heart murmurs and can be used in diagnosing systolic heart murmur. In comparison with the commercial medical machines used in tissue doppler imaging, the proposed system provides a lighter and cheaper solution.

V. CHIP DESIGN OF HEART SOUND CLASSIFYING ALGORITHM

The computation load of a smart device can be reduced using an edge computing method that transfers a part of the computing load from the smart device to the hardware. Therefore, a heart sound classifying chip is implemented. The chip can classify heart sounds without the assistance of ECG signals. The block diagram of ideal intelligent stethoscope system with the chip is illustrated in Figure 2.

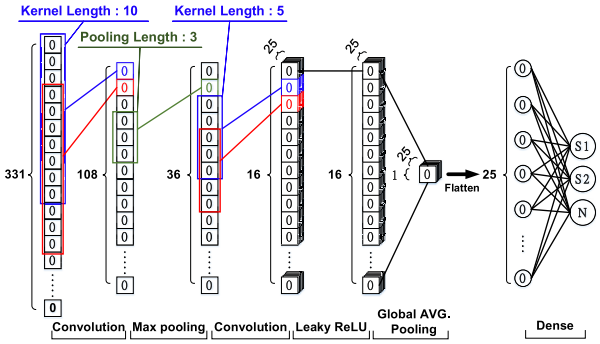

FIGURE 16. Data flow of CNN classification.

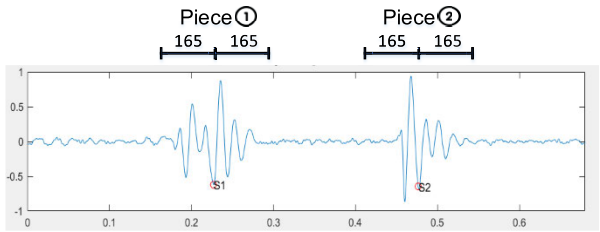

FIGURE 17. 331-point data pieces for CNN input.

In [20] and [21], artificial neural networks are used for the classification of heart sounds, but their algorithms are complex for hardware implementation. In this work, a light artificial intelligent (AI) model, which is a one-dimension convolutional neural network (CNN) [22], is realized. The CNN model has good performance and is a good tool for feature extraction. It facilitates hardware implementation compared with a recurrent neural network [23] and long short-term memory model [24]. Other models, such as deep neural networks [25], [26] and support vector machines usually involve complex pre-processing steps, which are not suitable for hardware implementation.

A. CHIP IMPLEMENTATION WITH CNN MODEL

The cost of hardware implementation can be reduced using a CNN model that is not too complex. Figure 16 shows that the CNN model used in the classification algorithm consists of six layers, including two convolutional layers, one max-pooling layer, one leaky rectified linear unit (ReLU) layer, one global average (AVG.) pooling layer, and one dense layer. The first layer is the convolutional layer with a kernel filter. The kernel length is 10 with a stride of 3. The second layer is the max-pooling layer with a length of 3, making the layer retain the biggest point every three points. The third layer is the second convolutional layer, which includes 25 kernel filters, and the kernel length is 5 with a stride of 2.

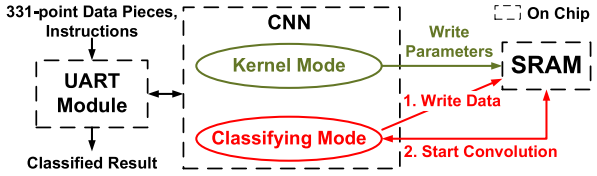

FIGURE 18. Structure and operation mode of hardware.

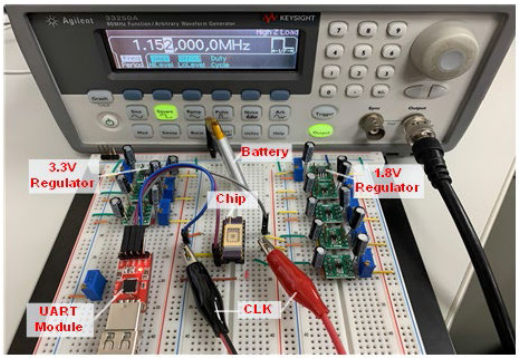

FIGURE 19. Measurement environment.

Therefore, the third layer generates the output data with a size of 16 × 25. In the fourth layer, the coefficient of leaky ReLU is initially set to 0.001, but it is slightly adjusted to 1/210 for hardware implementation. The fifth layer is the global average pooling layer, where the mean of the data in each feature map is calculated. As a result, the length of each feature map is shrunk to 1. Because the data are already one-dimensional and can be directly processed by the dense layer, the flattening step is not performed. The detailed formula of each layer and the principle of operation are discussed in [26].

The input of the CNN model is generated by the algorithm by pre-processing the raw heart sound data with two steps. First, the algorithm identifies heart sound peaks based on Shannon energy. Afterward, the algorithm divides the heart sound data into 331-point data pieces, including the data of the detected heart sound peak and 165-point data before and after the heart sound peak point, as shown in Figure 17. The dataset for the CNN model collected through clinical trials includes 3868 S1 peaks, 3747 S2 peaks, and 4671 noise peaks. The dataset is split into the training and the testing set with a ratio of 7:3. Afterward, the CNN model is trained by using the categorical cross-entropy loss function and the Nadam optimizer. The batch size and the number of epochs are set to 128 and 120, respectively. The proposed CNN model has a low hardware requirement. The model involves 239 parameters, and the model generates approximately 1,000 data points during operation. Therefore, the model can be implemented with integrated circuits.

B. CHIP IMPLEMENTATION

Figure 18 shows the structure of the heart sound classifying chip, which includes a universal asynchronous receiver/transmitter (UART) module for transmission, a CNN module for classification, and a static random access memory (SRAM) for data storage. The operation of the chip is also shown in Figure 18. The hardware is idle until an instruction is input through the UART. Once the instruction is received, the hardware enters the kernel mode to update CNN parameters or classifying mode for the classification of heart sound signals. The calculation performed in the hardware is based on fixed-point binary numbers. The size of input parameters and data is 16 bits, in which the input parameters are interpreted with 4-bit integers and 12-bit decimals, and the data are interpreted with 16-bit integers. In the SRAM, considering that the calculation with the fixed-point binary numbers is less accurate than the use of floating-point binary numbers, the data width is set to 32-bit for reducing calculation error.

TABLE 5. The testing result of the CNN model in the cloud server.

Confusion Matrix		Actual			
		Noise	S1	S2	Precision
Predicted	Noise	1344	10	9	98.6%
	S1	3	1117	50	95.5%
	S2	1	14	1138	98.7%
	Recall	99.7%	97.9%	95.1%	

TABLE 6. The testing result of the CNN model on the chip.

Confusion Matrix		Actual			
		Noise	S1	S2	Precision
Predicted	Noise	1357	5	1	99.6%
	S1	65	1080	25	92.3%
	S2	72	15	1066	92.5%
	Recall	90.8%	98.2%	97.6%	

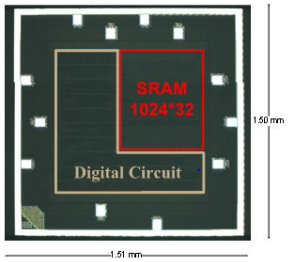

FIGURE 20. Chip microphotograph.

VI. MEASUREMENT RESULTS OF THE CHIP

As shown in Figure 19, a UART module, CP2102, is used to establish communication between the chip and computer

TABLE 7. Comparison of stethoscope system with state-of-the-art works.

	2019[27]	2020[28]	Eko[29]	2021[9]	2022[30]	This work	
Measured signal	Heart sound	Heart sound	Heart sound and ECG	Heart sound	Heart sound	Heart sound and ECG	
Hardware implementation	None	Yes	Yes	None	None	Yes	
Filters for heart sound	0–3k Hz	30–200 Hz	20–200 Hz or 20–2000 Hz	None	None	20–300 Hz and tube filter	
Wireless protocol	BLE 4.2	BLE 5.0	BLE 4.2	None	None	BLE 5.0	
Human trial	No	No	Yes	None	None	Yes	
Datasets for algorithm	None	None	Not available	PhysioNet[a]	PhysioNet[a] and MHSDB[b]	NCKUH clinical trials	
Classification precision	None	None	Not available	95.9%	98.3%	ECG-assisted 96.7%	Heart-sound-only 92.4%

[a]2016 PhysioNet/CinC Challenge [31]
[b]Michigan heart sound and murmur database [32]

for the renewal of the CNN parameters on the chip and monitoring the classification result of heart sound signals with the MATLAB. Tables 5 and 6 show the measurement results in the cloud server and on the chip. The F1 scores of the results are 96.7%–99.1% for Table 5 and 95%–95.2% for Table 6. The slight difference can be attributed to the error of fix-point calculation performed with the hardware.

The AI chip is fabricated in a 0.18-μm standard CMOS process with a maximum operation frequency of 1.152 MHz corresponding to the UART baud rate of 115,200. The power consumption of the chip is 93 μW. Figure 20 shows the microphotograph of the AI chip with dimensions of 1.51 mm $\times$ 1.50 mm. The SRAM occupies approximately one-third of the chip area, and the remaining area is occupied by digital circuits. Although more than 1,200 variables are required for the proposed CNN model, the space of some variables are reusable. Hence, a SRAM with size of 1,024 $\times$ 32 bits is sufficient.

VII. COMPARISON WITH STATE-OF-THE-ART WORKS

Table 7 shows the comparison between the proposed stethoscope system and the state-of-the-art works [27], [28], which can only acquire heart sound signals and cannot distinguish the locations of S1 and S2 from the heart sound signals. The proposed system can visualize both heart sound and ECG signals, thereby allowing convenient diagnosis. Although Eko's product [29] displays the heart sound and the ECG signals, its measured ECG signals are unstable because Eko's product integrates the measurement devices of heart sound and ECG into a single shell. Therefore, the characteristics of ECG signals change according to the auscultation site. Moreover, the adopted BLE 5.0 protocol has a higher energy efficiency than BLE 4.2 and other older versions of Bluetooth protocol. Additionally, only the proposed intelligent stethoscope system builds the frequency response model of the latex tube. Consequently, the properties of measured heart sounds are similar to those measured with the traditional stethoscope, and the characteristics of the heart murmurs are clear for assisting the diagnosis of cardiologists. In comparison with [9] and [30], which focus on the algorithms, the proposed ECG-assisted algorithm shows a comparable performance. Additionally, the light CNN algorithm on the chip shows the potential to assist physicians in real-time classifying the heart sounds without the ECG patch. Compared with these state-of-the-art works, the proposed system is more complete.

VIII. CONCLUSION

The present work has four main contributions. First, the proposed stethoscope system simultaneously measures the ECG and heart sound signals with independent devices, thus facilitating the auscultation and shortening the time of learning auscultation. Moreover, the combination of measured signals provides an accurate method for the detection of S1 and S2, which are important for both localizations of systolic and diastolic phases and heart murmur detection. Second, the usage of tube filter simulates the effect of latex tube in a traditional stethoscope and can recover the traditional waveforms from the signals measured with the digital stethoscope. Third, according to the analysis of the data collected in clinical trials, including the characteristics of heart sound signals measured on different auscultation sites and the results of wavelet analysis, the proposed system can provide enough evidence for the diagnosis of MR and AS. Fourth, the integrated circuits design of the classification algorithm reduces the computation effort of the smart device and shows the potential of VHD detection locally. In terms of the performance of proposed algorithm, the accuracy of ECG-assisted heart sound classification applied to normal heart sound signals reaches 100%, and the classification accuracy for the heart sound signals with heart murmur reaches 96.7%. The confusion matrix of heart murmur detection reveals a macro F1 score of 92.5%. The CNN-based heart sound classification implemented in the cloud server and on chip shows F1 scores of 96.7%–99.1% and 95%–95.2%, respectively. In comparison

with the state-of-the-art research and products, the proposed stethoscope system provides a more complete solution for the digital stethoscope. Moreover, in the proposed system, the independent measurement devices for the ECG and the heart sound provide flexibility for usage. Future works should improve the heart murmur detection algorithm to detect more kinds of heart murmur, and it should be integrated on chip to fit the concept of edge computing.

REFERENCES

[1] World Health Organization. *The Top 10 Causes of Death*. Accessed: Dec. 10, 2020. [Online]. Available: https://www.who.int/news-room/fact-sheets/detail/the-top-10-causes-of-death
[2] V. T. Nkomo, J. M. Gardin, T. N. Skelton, J. S. Gottdiener, C. G. Scott, and M. Enriquez-Sarano, "Burden of valvular heart diseases: A population-based study," *Lancet*, vol. 368, no. 9540, pp. 1005–1011, Sep. 2006.
[3] S. LaHaye, J. Lincoln, and V. Garg, "Genetics of valvular heart disease," *Current Cardiol. Rep.*, vol. 16, no. 6, p. 487, Jun. 2014.
[4] (2017). *3M Littmann, Cardiac Auscultation*. Accessed: Dec. 10, 2020. [Online]. Available: http://multimedia.3m.com/mws/media/1372905O/3mtm-littmannr-stethoscopes-auscultation-posters.pdf
[5] A. P. Yoganathan, R. Gupta, W. H. Corcoran, F. E. Udwadia, R. Sarma, and R. J. Bing, "Use of the fast Fourier transform in the frequency analysis of the second heart sound in normal man," *Med. Biol. Eng.*, vol. 14, no. 4, pp. 455–460, Jul. 1976.
[6] H. Nazeran, "Wavelet-based segmentation and feature extraction of heart sounds for intelligent PDA-based phonocardiography," *Methods Inf. Med.*, vol. 46, no. 2, pp. 41–135, 2007.
[7] S. Omran and M. Tayel, "A heart sound segmentation and feature extraction algorithm using wavelets," in *Proc. 1st Int. Symp. Control, Commun. Signal Process.*, 2004, pp. 235–238.
[8] P. S. Vikhe, S. T. Hamde, and N. S. Nehe, "Wavelet transform based abnormality analysis of heart sound," in *Proc. Int. Conf. Adv. Comput., Control, Telecommun. Technol.*, Dec. 2009, pp. 367–371.
[9] E. Messner, M. Zöhrer, and F. Pernkopf, "Heart sound segmentation—An event detection approach using deep recurrent neural networks," *IEEE Trans. Biomed. Eng.*, vol. 65, no. 9, pp. 1964–1974, Sep. 2018.
[10] S. Swarup and A. Makaryus, "Digital stethoscope: Technology update," *Med. Devices, Evidence Res.*, vol. 11, pp. 29–36, Jan. 2018.
[11] H. Ren, H. Jin, C. Chen, H. Ghayvat, and W. Chen, "A novel cardiac auscultation monitoring system based on wireless sensing for healthcare," *IEEE J. Translational Eng. Health Med.*, vol. 6, pp. 1–12, 2018.
[12] T. Xian-ting and Z. Zhi-dong, "Heart sound acquisition based on PDA and Bluetooth," in *Proc. 4th Int. Conf. Biomed. Eng. Informat. (BMEI)*, Oct. 2011, pp. 773–776.
[13] S.-Y. Lee, J.-H. Hong, C.-H. Hsieh, M.-C. Liang, S.-Y. Chang Chien, and K.-H. Lin, "Low-power wireless ECG acquisition and classification system for body sensor networks," *IEEE J. Biomed. Health Informat.*, vol. 19, no. 1, pp. 236–246, Jan. 2015.
[14] S. Majumder, L. Chen, O. Marinov, C. Chen, T. Mondal, and M. J. Deen, "Noncontact wearable wireless ECG systems for long-term monitoring," *IEEE Rev. Biomed. Eng.*, vol. 11, pp. 306–321, 2018.
[15] T. Wu, F. Wu, C. Qiu, J.-M. Redoute, and M. R. Yuce, "A rigid-flex wearable health monitoring sensor patch for IoT-connected healthcare applications," *IEEE Internet Things J.*, vol. 7, no. 8, pp. 6932–6945, Aug. 2020.
[16] N. Dey, A. S. Ashour, F. Shi, S. J. Fong, and R. S. Sherratt, "Developing residential wireless sensor networks for ECG healthcare monitoring," *IEEE Trans. Consum. Electron.*, vol. 63, no. 4, pp. 442–449, Nov. 2017.
[17] P. K. Sharma, S. Saha, and S. Kumari, "Study and design of a Shannon-energy-envelope-based phonocardiogram peak spacing analysis for estimating arrhythmic heart-beat," *Int. J. Sci. Res. Publications*, vol. 4, no. 9, pp. 1–5, Sep. 2014.
[18] V. Nivitha Varghees and K. I. Ramachandran, "Effective heart sound segmentation and murmur classification using empirical wavelet transform and instantaneous phase for electronic stethoscope," *IEEE Sensors J.*, vol. 17, no. 12, pp. 3861–3872, Jun. 2017.
[19] S. Lee, P. Huang, J. Chiou, C. Tsou, Y. Liao, and J. Chen, "Electrocardiogram and phonocardiogram monitoring system for cardiac auscultation," *IEEE Trans. Biomed. Circuits Syst.*, vol. 13, no. 6, pp. 1471–1482, Dec. 2019.
[20] T. Ölmez and Z. Dokur, "Classification of heart sounds using an artificial neural network," *Pattern Recognit. Lett.*, vol. 24, nos. 1–3, pp. 617–629, Jan. 2003.
[21] F. Li, M. Liu, Y. Zhao, L. Kong, L. Dong, X. Liu, and M. Hui, "Feature extraction and classification of heart sound using 1D convolutional neural networks," *EURASIP J. Adv. Signal Process.*, vol. 2019, no. 1, pp. 1–11, Dec. 2019.
[22] Y. Lecun, L. Bottou, Y. Bengio, and P. Haffner, "Gradient-based learning applied to document recognition," *Proc. IEEE*, vol. 86, no. 11, pp. 2278–2324, Nov. 1998.
[23] B. A. Pearlmutter, "Learning state space trajectories in recurrent neural networks," in *Proc. Int. Joint Conf. Neural Netw.*, Washington, DC, USA, 1989, pp. 365–372.
[24] S. Hochreiter and J. Schmidhuber, "Long short-term memory," *Neural Comput.*, vol. 9, no. 8, pp. 1735–1780, 1997.
[25] Y. Bengio, "Learning deep architectures for AI," *Found. Trends Mach. Learn.*, vol. 2, no. 1, pp. 1–127, 2009.
[26] J. Schmidhuber, "Deep learning in neural networks: An overview," *Neural Netw.*, vol. 61, pp. 85–117, Jan. 2015.
[27] H. Huang, D. Yang, X. Yang, Y. Lei, and Y. Chen, "Portable multifunctional electronic stethoscope," in *Proc. IEEE 3rd Inf. Technol., Netw., Electron. Autom. Control Conf. (ITNEC)*, Mar. 2019, pp. 691–694.
[28] J. Malwade, S. Sayyed, J. Nasir, Y. Parab, G. Narayanan, and S. Gupta, "Wireless stethoscope with Bluetooth technology," in *Proc. Int. Conf. Comput. Perform. Eval. (ComPE)*, Jul. 2020, pp. 168–172.
[29] Eko Devices Inc. *DUO ECG+Digital Stethoscope*. Accessed: Dec. 10, 2020. [Online]. Available: https://shop.ekohealth.com/products/duo-ecg-digital-stethoscope
[30] S. K. Ghosh, R. N. Ponnalagu, R. K. Tripathy, G. Panda, and R. B. Pachori, "Automated heart sound activity detection from PCG signal using time–frequency-domain deep neural network," *IEEE Trans. Instrum. Meas.*, vol. 71, pp. 1–10, 2022.
[31] A. L. Goldberger, L. A. N. Amaral, L. Glass, J. M. Hausdorff, P. C. Ivanov, R. G. Mark, J. E. Mietus, G. B. Moody, C.-K. Peng, and H. E. Stanley, "PhysioBank, PhysioToolkit, and PhysioNet: Components of a new research resource for complex physiologic signals," *Circulation*, vol. 101, no. 23, pp. e215–e220, Jun. 2000.
[32] R. Judge and R. Mangrulkar, "Heart sound and murmur library," Michigan Educ. Resour., USA, Tech. Rep. 120554, 2015. Accessed: May 13, 2023. [Online]. Available: http://www.med.umich.edu/lrc/psb/heartsounds/index.htm

SHUENN-YUH LEE (Senior Member, IEEE) was born in Taichung, Taiwan, in 1966. He received the B.S. degree from National Taiwan Ocean University, Keelung, Taiwan, in 1988, and the M.S. and Ph.D. degrees from National Cheng Kung University, Tainan, Taiwan, in 1994 and 1999, respectively.

He is currently a Distinguished Professor with the Department of Electrical Engineering, National Cheng Kung University. His research interests include the design of analog and mixed-signal integrated circuits, biomedical circuits and systems, artificial intelligence integrated circuits, low-power and low-voltage analog circuits, and RF front-end integrated circuits for wireless communications.

Dr. Lee is a member of the IEEE Circuits and Systems (CAS) Society, the IEEE Solid-State Circuits Society (SSCS), and the IEEE Medicine and Biology Society (EMBS). He is also a member of IEICE. He served as the Technical Program Chair (TPC) for the 2014/2015 International Symposium on Bioelectronics and Bioinformatics (ISBB) and the 2015 Taiwan and Japan Conference on Circuits and Systems (TJCAS). He served as the General Co-Chair for the 2022 IEEE Biomedical Circuits and Systems Conference (BioCAS) and the Organization Chair for the 2022 IEEE Asia Solid-State Circuits Conference (ASSCC). From 2013 to 2016, he serves as the Chairperson for the IEEE Solid-State Circuits Society Tainan Chapter. From 2016 to 2017, he serves as the Vice Chairperson for the IEEE Tainan Section. Since 2016, he serves as an Associate Editor for IEEE TRANSACTIONS ON BIOMEDICAL CIRCUITS AND SYSTEMS.

PO-HAN SU (Student Member, IEEE) was born in Chiayi, Taiwan, in 1993. He received the B.S. degree from National Cheng Kung University, Tainan, Taiwan, in 2015, where he is currently pursuing the Ph.D. degree with the Institute of Electrical Engineering.

His research interests include the design of analog integrated circuits, biomedical circuits and systems, and bio-signal processing algorithm.

YI-TING HSIEH (Graduate Student Member, IEEE) was born in Kaohsiung City, Taiwan, in 1997. He received the B.S. degree from National Cheng Kung University, Tainan, Taiwan, in 2019, where he is currently pursuing the Ph.D. degree with the Department of Electrical Engineering.

His research interests include analog front-end circuit, analog/mixed-signal integrated circuits, digital signal processing, and biomedical implantable systems.

SHENG-HSIN HUANG was born in Taichung, Taiwan, in 1995. He received the M.S. degree from National Cheng Kung University, Tainan, Taiwan, in 2021. His research interests include bio-system integration, phonocardiogram, digital circuit design, and AI algorithm.

I-PEI LEE was born in Tainan, Taiwan, in 1998. She received the B.S. degree from the School of Medicine, Kaohsiung Medical University, Kaohsiung, Taiwan, in 2022.

She is currently a Doctor in post-graduate year training with National Cheng Kung University Hospital. Her research interest includes cardiovascular diseases, including arrhythmias, cardiac surgery, and cardiac implantable electric devices.

JU-YI CHEN was born in Tainan, Taiwan, in 1974. He received the M.S. degree from Chang Gung University, Taoyuan City, Taiwan, in 1999, and the Ph.D. degree from National Cheng Kung University, Tainan, in 2013.

Since 2021, he has been a Professor with the Department of Internal Medicine, National Cheng Kung University. His research interest includes cardiovascular diseases, including arrhythmias, hypertension, arterial stiffness, and cardiac implantable electric devices.